Proceedings of the 29th Annual International
Conference of the IEEE EMBS
Cité Internationale, Lyon, France
August 23-26, 2007.

Poloxamer 188 Reduces Axonal Beading Following Mechanical Trauma to Cultured Neurons

Devrim Kilinc, *Member, IEEE*, Gianluca Gallo, and Kenneth Barbee

***Abstract*—Diffuse axonal injury (DAI), a major component of traumatic brain injury, is a progressive event that may lead to secondary neuronal death. DAI is thought to be initiated by mechanically-induced increases in axolemmal permeability resulting in disruption of the cytoskeleton and blockade of axonal transport. We report an *in vitro* model that mimics important features of DAI observed *in vivo*. We induced fluid shear stress injury (FSSI) on cultured primary chick forebrain neurons and characterized the resulting structural and morphological changes. In addition, we tested the post-injury effect of Poloxamer 188 (P188), a tri-block co-polymer that is known to promote resealing membrane pores. We found that FSSI induces axonal beading, the "hallmark" morphology of DAI. Furthermore, beads co-localized with microtubule disruption, also characteristic of DAI. P188 reduced axonal beading to control levels indicating that axolemma integrity is an excellent target for therapeutic interventions.**

I. Introduction

TRAUMATIC brain injury (TBI) results in a substantial portion of fatal injuries and may lead to neurological dysfunction in case of survival [1]. Diffuse axonal injury (DAI), the diffuse form of TBI, displays widespread damage in the white matter and is thought to result from inertial forces applied on the head [2]. DAI is a continuum of neurochemical and morphological changes, characterized by axonal bead formation leading to disconnection from target tissue and cell death [3]. Understanding the cell biological mechanisms underlying DAI is important for identifying potential therapeutic targets for *in vivo* intervention.

Formation of axonal swellings, or beads, is the morphological hallmark of DAI pathology [4]. Beading is reflective of accumulation of proteins and membrane-bound organelles at distinct locations along the axon due to impaired axonal transport [5]. Since axons depend on motor protein-driven transport along microtubule tracks [6], a direct relationship between microtubule loss and bead formation is suspected [5], but has not been demonstrated. Focal disruption of the axonal cytoskeleton may result in focal impairment of axonal transport leading to bead formation.

Manuscript received April 16, 2007. This work was supported by Drexel University GRID Fellowship. D. Kilinc is with the Drexel University, Philadelphia, PA 19104 USA (phone: 215-762-2070; fax: 215-762-2081; e-mail: devrim.kilinc@drexel.edu).

G. Gallo is with Drexel University School of Medicine, Philadelphia, PA 19129 USA (e-mail: Gianluca.Gallo@DrexelMed.edu).

K. A. Barbee is with the School of Biomedical Engineering, Science, and Health Systems, Drexel University, Philadelphia, PA 19104 USA (e-mail: barbee@cbis.ece.drexel.edu).

Mechanoporation, the generation of transient membrane pores due to mechanical deformation, has been suggested to initiate DAI [2]. Increase in axolemmal permeability [7] and sharp rise in intracellular calcium ion concentration ($[Ca^{2+}]_i$) following injury [8] suggest ion influx through membrane pores. Ca^{2+} is considered as a key factor in TBI pathology, since calpains, Ca^{2+}-activated proteases, can degrade various cytoskeletal proteins including tubulin (reviewed in [3]).

Poloxamer 188 (P188) is an amphiphilic tri-block co-polymer capable of sealing cell membranes after heat shock, electroporation, and radiation [9]. Membrane resealing properties of this surfactant provide a tool for assessing the membrane damage in the trauma-induced axonal pathology. We have recently demonstrated the ability of P188 to protect neuron-like PC2 cells from trauma-induced cell death by acutely repairing their membranes [10]. P188 treatment not only prevented necrosis, but also significantly decreased apoptosis, suggesting that mechanoporation was initiating the signaling cascades leading to apoptosis [11].

In the current study, we examine the relationship between mechanical trauma and subsequent axonal pathology. We describe an *in vitro* model of axonal injury initiated by fluid shear stress and demonstrate that axons mimic the hallmarks of *in vivo* DAI. Traumatic injury results in axonal bead formation and localized microtubule disruption. Finally, we show that treatment with P188 post-injury prevents axonal bead formation.

II. Methods

A. Cell Culture

Embryonic day 8 chick forebrain neurons were harvested, dissociated and plated on indexed German glass coverslips (Bellco Glass, Vineland, NJ) at a concentration of 1.5×10^4 cells·cm^{-2} [12]. Coverslip surfaces were pre-treated to promote attachment [13]. Indexed coverslips were used for tracking sets of individual neurons over time via phase contrast microscopy and *post hoc* immunocytochemistry. Cultures were maintained in supplemented M199 medium (Invitrogen, Carlsbad, CA) and incubated (5% CO_2; 37°C) for 4-6 days before experimentation. Culture medium was changed every other day. HEPES buffered, CO_2-independent, supplemented Ham's F12 medium (Invitrogen) was used as experimental medium during live imaging experiments.

B. Experimental Procedure

The controlled shear stress device (CSSD) is a cone-and-plate viscometer-based apparatus that applies uniform shear stress over the coverslip through the controlled rotation of the cone (Figure 1) [14]. When used with high onset rates, CSSD induces fluid shear stress injury (FSSI) in the neural culture [10]. A shear impulse of 45 dyn·cm^{-2} with 20 ms onset time was used to induce FSSI. Sham (uninjured) controls underwent the exact protocol except without the cone rotation. A stage heater (NevTek, Burnsville, VA) maintained constant temperature (37°C) and images were taken with an inverted Nikon Diaphot Eclipse TE300 microscope (Optical Apparatus, West Chester, PA). P188 (Pluronic acid F-68, Sigma, St. Louis, MO) was dissolved in experimental medium and applied to neurons at 5 min post-injury (final concentration: 100μM).

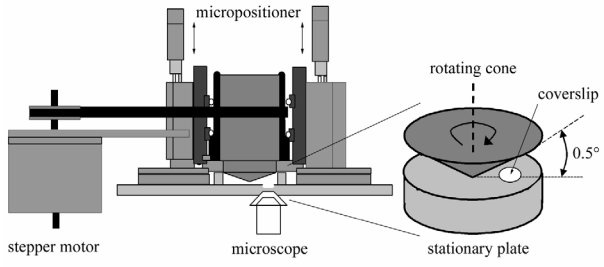

Fig. 1. Controlled shear stress injury device [14]. Note that the cone angle is exaggerated in the drawing.

C. Quantification of Beading

Images were obtained before and 60 min after the injury. Axonal beading (Fig. 2) is quantified by counting beads that emerged during the post-injury period and normalizing this number by the length of the axon. To eliminate the human factor in this process, a Matlab (MathWorks, Natick, MA) program was written to categorize beads. This program takes a phase contrast image of a neuron as input and returns a beading vector and a categorized bead count. The pixel values of the original image (Fig. 3A) are assigned to a two-dimensional matrix. With an interactive process, unrelated objects are removed from the image (Fig. 3B). A complement (pixel values subtracted from white) image is created (Fig. 3C) and transformed to a black-and-white (BW) matrix using an interactive subroutine (Fig. 3D). Another interactive subroutine helps the user pick neuronal areas from the BW image (Fig. 3E). Due to variations in the background of the original image, BW neuron is usually segmented. Segments are connected by user-added dots and by utilizing intrinsic dilation and erosion functions of Matlab (Fig. 3F). Another intrinsic Matlab function calculates the so-called "shaft" of the neuron (Fig. 3G) and interactively lets the user first to select the pixels to be discarded and then to indicate the desired portion of the shaft (Fig. 3H). The shaft vector contains the indices of pixels that make up the shaft. For each point along the shaft, a disk whose radius varies from 1 to 10 is superimposed

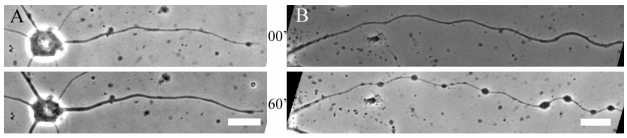

Fig. 2. Phase contrast images of an injured and sham neuron. Beads develop in the injured neuron (B) over the course of 60 minutes, while uninjured (sham) axon maintains its morphology (A). Bars = 20μm.

with the BW neuron image and the biggest radius that overlaps > 85% with the neuronal area is recorded to the beading matrix. Therefore, the beading matrix contains the thickness of the axon (or the bead radius) for each point along the shaft. Pixels, whose radii are smaller than twice of the average radius of the entire shaft, are filtered out. Pixels in close proximity to local maxima are also eliminated. Beading matrix, average radius before filtering, and length of the axon is then used to obtain a single number to represent the "beading state" of the corresponding axon. The difference in these calculated numbers for the same axon pre-injury and at 60 min post-injury is considered as the increase in beading and used for comparison. We determined that both manual and software-based methods produced similar results.

D. Visualization of Cytoskeleton

Cultures were fixed using simultaneous fixation and extraction method [15] that allows extracting free tubulin out of the axoplasm while fixing microtubules. Fixed cultures were treated with 2 mg/ml sodium borohydride (Sigma) and stained to reveal tubulin with DM1A anti-tubulin (1:100, Sigma). Images were acquired using a Zeiss 200M microscope (Zeiss, Gottingen, Germany) and captured with AxioVision software (Zeiss). Microtubule mass along the axon, measured by tubulin staining intensity, was quantified with a Matlab-based program. This program is similar to the beading program up to the point where the axon shaft is created, except that the complement image is

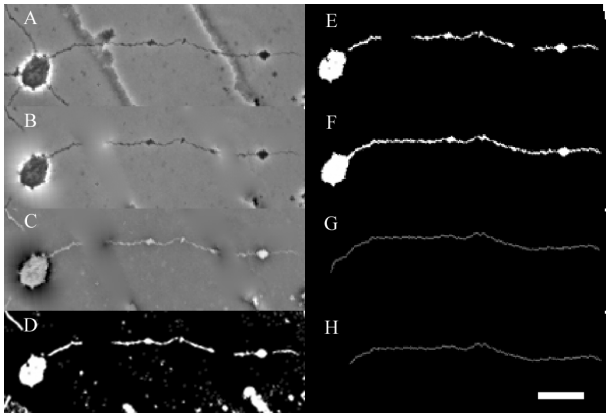

Fig. 3. Steps of computer based beading quantification algorithm. Briefly, the original image (A) is cleaned (B), reversed (C), and thresholded to black and white (D), before the user picks neuronal regions (E). Once the connectivity is reached (F), the spine is created (G) and trimmed to reflect the axon (H). Black and white image and the spine are then used to determine beading vector. Bar = 20μm.

not required. Intensity values of the raw image at pixels along the shaft are stored into the intensity matrix. To obtain a similar structure to the beading matrix, intensity values are binned using a function that spans an interval between the average intensity and minimum intensity and assigns a score on a 1 to 10 scale for each pixel along the shaft. Higher scores mean low intensity values. This matrix is further filtered and categorized using same sub-functions explained above.

To analyze co-localization of axonal beads with regions of low microtubule staining intensity, an intensity scale was created between the minimum and the average values of intensity among the pixels of the shaft. The decrease in intensity of individual pixels, representing microtubule loss, was then expressed as a percentage of this range.

E. Statistical Analysis

Data were expressed as mean ± standard error of the mean (SEM). Statistical analysis was performed using single way analysis of variance, followed by Tukey's *post hoc* test to determine significance values between different groups.

III. Results

A. Mechanical Injury Induces Axonal Beading

Cultured chick forebrain neurons were subjected to FSSI. Live imaging of injured neurons revealed the gradual appearance of axonal beading (Figure 2). Beads started to form as early as 5 min post-injury throughout the length of the axon, whereas the majority of beads formed after 20 min. Beads gradually increased in size and in number while the connecting segments of the axon become thinner and eventually disintegrate (not shown). Images taken pre-injury and 60 min post-injury were analyzed. Axonal beading was significantly higher in injured neurons compared to sham controls also verified by software-based image analysis (Figure 4). Axonal beads are usually present in low amounts in sham and incubator controls (data not shown), reflecting packets of axonal transport observed in healthy neurons [16].

B. Beads Co-localize with Microtubule Discontinuities

Microtubules are the tracks for the axonal transport of organelles [6]. Accumulation of organelles along axons during bead formation is likely to be indicative of a block of axonal transport. We investigated whether FSSI-induced axonal beading was related to changes in the cytoskeleton by staining microtubules. No effect of FSSI on total microtubule levels was detected in the post-injury period during which beads form (data not shown; n = 67; p = 0.46). However, analysis of individual axons revealed a relation between local decreases in axonal microtubule mass and the presence of beads (Figure 5A). Co-localization of beads and local minima of microtubule staining intensity was analyzed by software-based analysis. Figure 5B shows a plot of microtubule intensity loss relative to bead size. Intensity loss

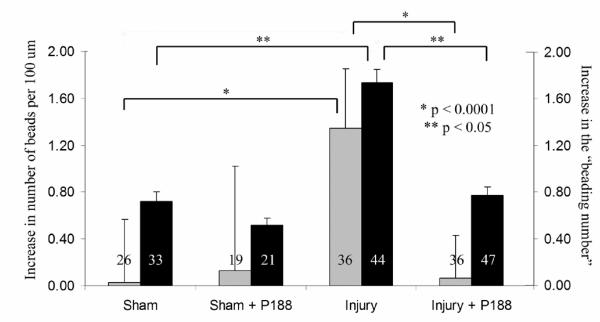

Fig. 4. Axonal beading at 1h post-injury. Beading is measured by the number of post-injury beads divided by axon length (light bars) and by Matlab-based program (dark bars). Beading was higher in the injury group compared to sham controls. P188 has no effect on sham controls but significantly reduces beading in the injured neurons. N is displayed on bars. Error bars represent SEM.

for each bead location is given by the percentage decrease from the average intensity of the corresponding axon. Our findings indicate that FSSI results in localized disruption of axonal microtubule. The localized sites of microtubule disruption, in turn, correlated with axonal beads.

C. Post-injury P188 Treatment Reduces Axonal Beading

We tested whether P188 can block the formation of axonal beads in response to FSSI. For a reagent to be useful in a therapeutic context, it has to be applied after the injury. Moreover, the timing of P188 treatment, in our model, is relevant since most of the beads emerged 5 min after injury (not shown). Treatment with P188 blocked bead formation in response to FSSI (Figure 4). The block of bead formation by P188 was confirmed by observer-independent computer assisted analysis of bead formation ($p<0.05$, see Methods).

IV. Discussion

Elucidation of the mechanism of DAI provides opportunities for therapeutic intervention. Axonal beading was observed in postmortem human DAI [17] and in *in vivo* injury models [18]. Our *in vitro* injury model mimics this hallmark morphology in response to mechanical trauma on cultured primary neurons. Therefore, it is a promising tool for the study of the mechanisms of mechanically induced DAI and to test novel treatment strategies at the cellular level. Indeed, we demonstrate for the first time that using a membrane resealing agent following injury blocks the

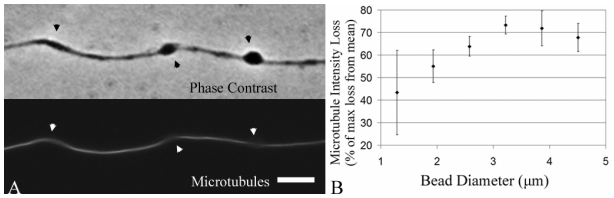

Fig. 5. Beads co-localize with microtubule discontinuities in an injured axon (A). Loss in the microtubule intensity increases with the bead diameter. N = 192 beads. Error bars represent SEM (B). Bar = 20μm.

formation of axonal beads.

Axonal transport depends on molecular motors associated with microtubules [6]. Therefore, impaired axonal transport following TBI is likely related to structural changes in the axonal microtubule array. Localized and rapid microtubule loss and accumulation of organelles at beads along undisrupted axons has been shown following *in vivo* injury [5]. It is remarkable that our *in vitro* model mimics the localized disruption of the microtubule array observed *in vivo*, indicating that this phenomenon is due to mechanisms intrinsic to the axon and not due to injury-induced extracellular events.

The mechanisms underlying the heterogeneous disruption of microtubules by injury are unknown. A heterogeneous decrease in the membrane Ca^{2+}-ATPase activity was shown following *in vivo* injury [19] suggesting heterogeneous [Ca^{2+}] along the axon. Calpain is Ca^{2+}-activated enzyme that can degrade tubulin [3]. Thus, heterogeneity in Ca^{2+}-dependent calpain activation might underlie localized disruption of microtubules. Alternatively, local microtubule loss might be due to local differences in their structural properties, leaving certain locations more vulnerable to degradation.

Focal impairment of axonal transport has been shown to occur 60 min after mild to moderate TBI, while beading has been observed between 6 to 12h after *in vivo* injury [2]. The progression of injury to the human brain is remarkably slower than in other experimental systems (for a review see [3]), indicating the possibility of a large window of opportunity for therapeutic intervention [20]. Damage to cell membranes can be reversed by P188 via resealing of membrane pores [9], [10]. The ability of block co-polymer surfactants to provide protection has also been tested using *in vivo* injury models. In impact acceleration injury to rat, intravenous injection of polyethylene glycol reduced injury-related dye accumulation to control levels [21]. Furthermore, subcutaneous P188 injected at 6h post-injury promoted structural and functional recovery following spinal cord injury [22]. In conjunction with our *in vitro* studies, these reports indicate that tri-block co-polymer surfactants may be used *in vivo* to mitigate the effects of DAI.

Our current results reveal that mechanical injury induces axonal beading, the hallmark of DAI, in cortical neurons and that post-injury P188 treatment prevents axonal bead formation. Therefore, P188 is a promising agent to block the neuropathological sequelae of DAI. The *in vivo* potential of P188 to block DAI should be addressed in future work.

REFERENCES

[1] A. E. Davis, "Mechanisms of traumatic brain injury: biomechanical, structural and cellular considerations," *Crit. Care. Nurs. Q.*, vol. 23, pp. 1–13, Nov. 2000.

[2] T. A. Gennarelli, L. E. Thibault, and D. I. Graham, "Diffuse axonal injury: an important form of traumatic brain damage," *Neuroscientist*, vol. 4, pp. 202–215, May 1998.

[3] M. Gaetz, "The neurophysiology of brain injury," *Clin. Neurophysiol.*, vol. 115, pp. 4–18, Jan. 2004.

[4] J. T. Povlishock, and C. W. Christman, "The pathobiology of traumatically induced axonal injury in animals and humans: a review of current thoughts," *J. Neurotrauma*, vol. 12, pp. 555–564, Aug. 1995.

[5] W. L. Maxwell, "Histopathological changes at central nodes of Ranvier after stretch-injury," *Microsc. Res. Tech.*, vol. 34, pp. 522–535, Aug. 1996.

[6] M. Coleman, "Axon degeneration mechanisms: commonality amid diversity," *Nat. Rev. Neurosci.*, vol. 6, pp. 889–898, Nov. 2005.

[7] E. H. Pettus, C. W. Christman, M. L. Giebel, and J. T. Povlishock, "Traumatically induced altered membrane permeability: its relationship to traumatically induced reactive axonal change," *J. Neurotrauma*, vol. 11, pp. 507–522, Oct. 1994.

[8] M. C. LaPlaca, V. M. Lee, and L. E. Thibault, "An in vitro model of traumatic neuronal injury: loading rate-dependent changes in acute cytosolic calcium and lactate dehydrogenase release," *J. Neurotrauma*, vol. 14, pp. 355–368, June 1997.

[9] S. A. Maskarinec, G. Wu, and K. Y. Lee, "Membrane sealing by polymers," *Ann. N. Y. Acad. Sci.*, vol. 1066, pp. 310–320, Dec. 2005.

[10] G. Serbest, J. Horwitz, and K. A. Barbee, "The effect of poloxamer-188 on neuronal cell recovery from mechanical injury," *J. Neurotrauma*, vol. 22, pp. 119–132, Jan. 2005.

[11] G. Serbest, J. Horwitz, M. Jost, and K. A. Barbee, "Mechanisms of cell death and neuroprotection by poloxamer 188 after mechanical trauma," *FASEB J.*, vol. 20, pp. 308–310, Feb. 2006.

[12] S. R. Heidemann, M. Reynolds, K. Ngo, and P. Lamoureux, "The culture of chick forebrain neurons," *Methods Cell. Biol.*, vol. 71, pp. 51–65, July 2003.

[13] D. M. Geddes, M. C. LaPlaca, and R. S. Cargill, "Susceptibility of hippocampal neurons to mechanically induced injury," *Exp. Neurol.*, vol. 184, pp. 420–427, Nov. 2003.

[14] B. R. Blackman, K. A. Barbee, and L. E. Thibault, "In vitro cell shearing device to investigate the dynamic response of cells in a controlled hydrodynamic environment," *Ann. Biomed. Eng.*, vol. 28, pp. 363–372, June 2000.

[15] G. Gallo, and P. G. Letourneau PG, "Different contributions of microtubule dynamics and transport to the growth of axons and collateral sprouts," *J. Neurosci.*, vol. 19, pp. 3860–3873, May 1999.

[16] E. Koenig. S. Kinsman, E. Repasky, and L. Sultz, "Rapid mobility of motile varicosities and inclusions containing alpha-spectrin, actin, and calmodulin in regenerating axons in vitro," *J. Neurosci.*, vol. 5, pp. 715–729, Mar. 1999.

[17] S. J. Strich, "Shearing of nerve fibres as a cause of brain damage due to head injury," *Lancet*, vol. 2, pp. 443–448, Aug. 1961.

[18] T. A. Gennarelli, L. E. Thibault, J. H. Adams, D. I. Graham, C. J. Thompson, and R. P. Marcincin, "Diffuse axonal injury and traumatic coma in the primate," *Ann. Neurol.*, vol. 12, pp. 564–574. Dec. 1982.

[19] W. L. Maxwell, B. J. McCreath, D. I. Graham, and T. A, Gennarelli "Cytochemical evidence for redistribution of membrane pump calcium-ATPase and ecto-Ca-ATPase activity, and calcium influx in myelinated nerve fibres of the optic nerve after stretch injury," *J. Neurocytol.*, vol. 24, pp. 925–942, Dec. 1995.

[20] M. S. Grady, M. R. McLaughlin, C. W. Christman, A. B. Valadka, C. L. Fligner, and J. T. Povlishock, "The use of antibodies targeted against the neurofilament subunits for the detection of diffuse axonal injury in humans," *J. Neuropathol. Exp. Neurol.*, vol. 52, pp. 143–152, Mar. 1993.

[21] A. O. Koob, B. S. Duerstock, C. F. Babbs, Y. Sun, and R. B. Borgens, "Intravenous polyethylene glycol inhibits the loss of cerebral cells after brain injury," *J. Neurotrauma*, vol. 22, pp. 1092–1111, Oct. 2005.

[22] R. B. Borgens, D. Bohnert, B. Duerstock, D. Spomar, and R. C. Lee, "Subcutaneous tri-block copolymer produces recovery from spinal cord injury," *J. Neurosci. Res.*, vol. 76, pp. 141–154, Apr. 2004.